Characteristics of a silicon carbide field emission array under pre-breakdown conditions

© V.A. Morozov,[1] N.V. Egorov,[1] V.V. Trofimov,[1] K.A. Nikiforov,[1] I.I. Zakirov,[2] V.M. Kats,[1] V.A. Ilyin,[3] A.S. Ivanov[3]

[1] St. Petersburg State University,
St. Petersburg, Russia
[2] Bonch-Bruevich St. Petersburg State University of Telecommunications,
St. Petersburg, Russia
[3] St. Petersburg State Electrotechnical University „LETI“,
St. Petersburg, Russia
e-mail: v.morozov@spbu.ru

This study assesses promising field electron sources based on silicon carbide monolithic field emission array (FEA). FEA is fabricated on single-crystal wafers of silicon carbide (0001C) 6H-SiC of n-type conductivity using the technology of two-stage reactive ion etching in $SF_6/O_2/Ar$ atmosphere. To implement conditions close to breakdown, an experimental setup based on high-voltage narrow pulses generating device GKVI-300 was used. A series of nanosecond voltage pulses with amplitudes from 120 to 250 kV was generated. To study the characteristics of the FEA in the pre-breakdown state, the beam of field emitted electrons was separated from the ion torch or cathode plasma, formed in the following breakdown phases, by placing a 50-μm-thick titanium foil under zero potential into the interelectrode gap. Current-voltage characteristics of peak-currents vs. peak-voltages passing through the foil are close to rectilinear in the Fowler−Nordheim coordinates. The current-voltage characteristics plotted for each of the pulses along increasing and decreasing branches show a discrepancy (hysteresis). After the experiments, the silicon carbide cathode FEA was studied in a scanning electron microscope.

Keywords: field electron emission, field emitter array, silicon carbide, pre-breakdown, high-voltage narrow pulses.

Introduction

In the current international competitive environment focused on solving problems in the field of creating an electronic component base (ECB), there is no doubt that the formation of a silicon carbide industry in Russia as one of the priority areas in solving the problems of import substitution of electronic components and ensuring parity in technologies that determine the scientific and technological competitiveness and state security [1]. In this regard, silicon carbide field emission structures were developed at the St. Petersburg State Electrotechnical University „LETI“ formed by various technological methods [2].

The most important element of any electrovacuum device is the source of electrons (cathode). Efficient field emission cathodes are still the subject of intense research [2–5]. Silicon carbide can be classified as a promising material for field emission electronics, primarily due to its high thermal conductivity and mechanical strength. Resistance to chemical and radiation effects should be considered an additional advantage of SiC. These circumstances make it possible to forecast the creation of silicon carbide-based microcathodes with field emission, which combine a high emission current density, stability of emission characteristics, and acceptably low values of the electric field strength of the onset of emission, which is important from a practical point of view.

The combination of advantages of field-electronic cathodes, including those under consideration, determines the prospects for their use in various electronic devices, for the effective operation of which cathode emission studies are carried out [6–10].

In this paper, we study a promising source of field electron emission based on microsized monolithic matrix cathodes [2]. As mentioned above, silicon carbide has many advantages for use as a material for emission sources: high values of the modulus of elasticity (and, as a consequence, structural rigidity) and stability of the surface topography; high values of thermal conductivity, allowing to significantly expand the range of operating temperatures; critical electric field strength of the order of 2 MV/cm as an important aspect in order to avoid transition to explosive emission. The monolithic structure of silicon carbide matrix cathodes contributes to the stability of field emission, since there are no weak points in the form of interfaces between nanostructures and the substrate, which negatively affect the ability to withstand vibration loads, ponderomotive forces, thermal effects, etc. The study of extreme modes of

operation of this cathode, such as the mode of explosive emission (pre-breakdown and breakdown conditions), is relevant.

1. Experimental setup and research technique

To study pre-breakdown and breakdown phenomena, an experimental setup based on the generator of short high-voltage pulses GKVI-300 (Fig. 1) with the following parameters was used: energy $W = 9-125$ J, voltage amplitude $U = 120-250$ kV, voltage pulse duration $\tau = 30-100$ ns. The matrix cathode used in the experiments is made in the form of a rectangular plate with dimensions $5 \times 5 \times 1$ mm, attached to a cylindrical rod. Matrix multipoint emitters are fabricated at LETI on single-crystal n-type $6H$-SiC (0001C) silicon carbide wafers using the technology of two-stage reactive ion etching in an SF_6O_2/Ar atmosphere [2]. Two-stage microdimensional matrix structures according to the manufacturing technology have a two-scale detailing of the working surface: the upper faces of the pedestals in the form of parallelepipeds with a base of $10 \times 10\,\mu$m with a step of $10\,\mu$m represent details of the first scale level, on which individual emission centers are created due to small tips, the details of the second scale level.

In the experiments, a voltage pulse applied to the electrodes was measured using a capacitive voltage divider, and the current was measured using a Rogowski coil.

In Ref. [11], four phases of current formation during vacuum breakdown were considered: the first phase is pre-breakdown, which consists in heating the emitter by field emission current, the second phase is the explosive destruction of the emitter and a sharp increase in current , the third phase is a relatively slow increase in current due to the emission of electrons from the cathode plasma, the fourth phase is an increase in current after the plasma bridges the vacuum gap. In Ref. [12] it is shown that the breakdown delay time determined by the first and second phases is a few nanoseconds (which corresponds to [9]), and the main delay time is determined by the third phase –
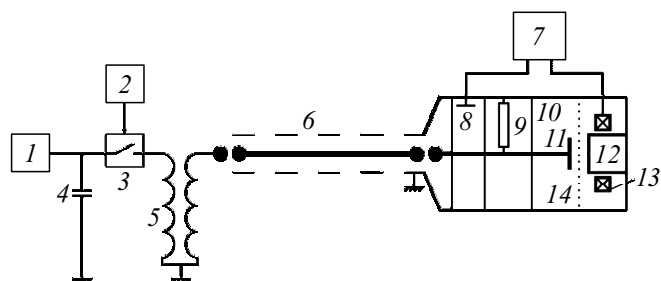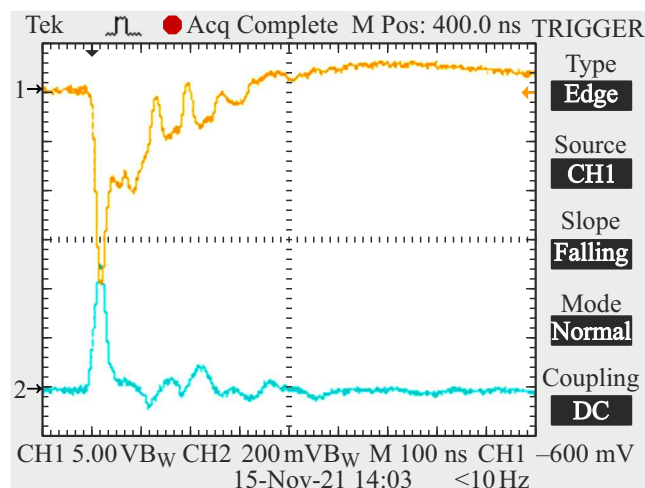
Figure 2. Characteristic oscillograms of voltage 1 and current 2 pulses.

it is the time of flight of the cathode plasma during the breakdown of the cathode−anode gap, its velocity being $(0.22-1.43) \cdot 10^5$ m/s [12]. The breakdown discharge delay time is basically the time of plasma passage to the anode, and a wide range of plasma velocity change is determined by the intensity of the electric field between the cathode and anode, as well as the state of the electrode surface [12].

In the course of experiment carried out with a large interelectrode gap of the order of 13 mm in the pulsed mode, all phases of breakdown development were recorded. The pulse shown in Fig. 2 is the first and second breakdown phases together. Since the main interest in this work is the characteristics of the studied matrix cathode in the pre-breakdown and breakdown states, it was necessary to separate the beam of field-emitted electrons of the first and second phases from the ion plume or cathode plasma formed at the next breakdown phases. For this purpose, a titanium foil (Fig. 1) with a thickness of $50\,\mu$m under zero potential was placed in the interelectrode gap, through which the transmission coefficient for field-emitted electrons is ~ 10, and the cathode plasma practically does not penetrate.

2. Experimental results and their discussion

2.1. CVC of a multi-tip flat silicon carbide cathode

As a result of experiments in the range of voltage amplitudes from 120 to 250 kV, 6 oscillograms of voltage and current pulses were recorded. One of the characteristic oscillograms is shown in Fig. 2.

Current-voltage characteristics (CVCs) were plotted using the pulse amplitudes in conventional coordinates (Fig. 3) and Fowler−Nordheim coordinates (Fig.-4).
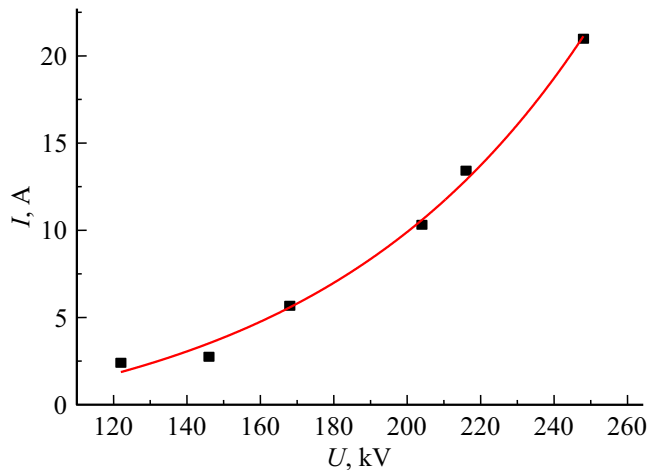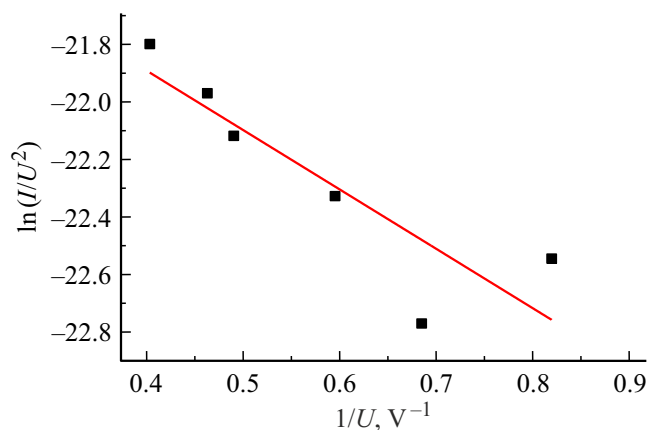
Figure 1. Schematic diagram of the experimental setup: *1* — charger, *2* — spark gap control circuit, *3* — spark gap, *4* — capacitor, *5* — pulse transformer, *6* — forming line, *7* — oscilloscope, *8* — capacitive divider, *9* — load resistor, *10* — vacuum chamber, *11* — cathode, *12* — electron collector, *13* — Rogowski coil, *14* — titanium foil.

Figure 3. BAX.

Figure 4. CVC in the Fowler−Nordheim coordinates
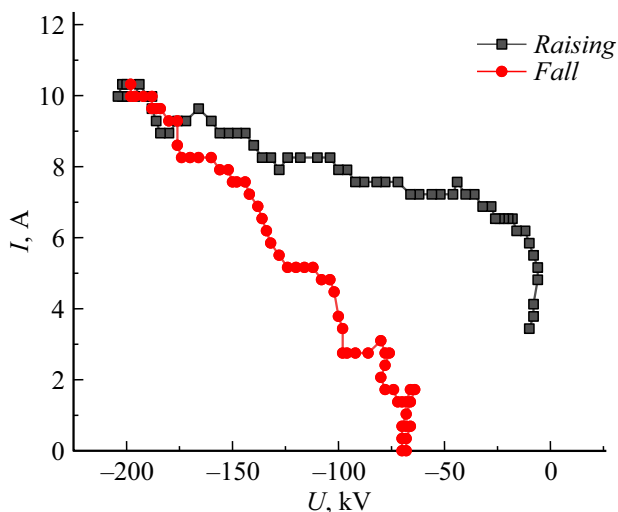

Figure 5. Typical CVC of a single pulse.

Note that the CVC plotted in the Fowler−Nordheim coordinates has a form that is close to rectilinear.

Analysis was carried out and the CVCs were plotted for each of the six measured voltage and current pulses tracing the rise and fall of the pulses. Figure 5 shows these characteristics for one pair of voltage and current pulses.

Analysis of the characteristics shows the discrepancy between the ascending and descending branches. It can be assumed that if no changes in the matrix morphology occurred during the rise in the voltage at the pulse leading edge, the CVCs for the pulse leading and trailing edges would coincide. However, in fact, they do not coincide, which can be considered an evidence for a change in conditions on the working surface of the cathode at the pulse leading edge, including morphology. This fact was reported in Ref. [13].

2.2. Investigation of the silicon carbide matrix using a scanning electron microscope (SEM)

After the experiments, the silicon carbide cathode was examined using a SEM (Zeiss Merlin with a GEMINI-II electron column based on a field emission cathode and a completely oil-free vacuum system; two detectors of secondary electrons were involved in the measurements: an Everhart−Thornley SE2 detector and an intralens In-Lens detector). Figure 6, *a* shows a general view of the matrix after the experiment; traces of explosions and a change in the surface morphology are visible. In Fig. 6, *b* footprints of a change in the matrix structure are observed, which affect not only the surface of the pedestals with microtips, but also penetrate deep into the main substrate. In Fig. 6, *c* a crater is shown, which could result from explosive electron emission. Explosive emission in some areas may indicate that in these areas there were either strong deviations from the average parameters of microtips, or a local change in the properties of the matrix due to the impact of sputtered particles. These particles were sputtered with cathode plasma from titanium foil, which served to cut it off, or from the foil holder. The latter was confirmed by traces of titanium and stainless steel found on the surface of the matrix.

Figure 7, *a* shows an example of delamination of emitting pedestals with microtip arrays. Fig. 7, *b* illustrates an example of saving the operational structure. In this case, a sufficiently high percentage of pedestals retains the original morphology, but microtips on pedestals are seen blunted. Figure 7, *c* shows an image of the matrix edge. It also shows the rounding of initially sharp edges, most likely caused by the decomposition of the cathode material during electron emission (silicon carbide of any polytype modification does not have a melting phase; the decomposition temperature is $2830°C$).

Having examined the SEM images of the silicon carbide matrix, we can conclude that both the edge of the matrix and its surface worked during the experiment. When the interelectrode distance is macroscopic, an increase in the electric field strength occurs at the edge of the matrix cathode (the results of modeling the diode configuration
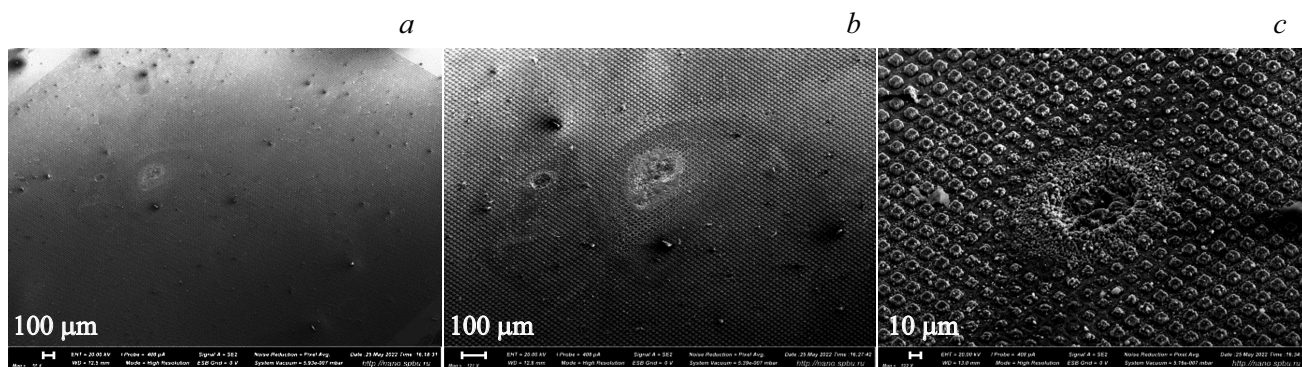
Figure 6. SEM image of the silicon carbide matrix after the experiment: *a* — general view of the matrix; *b* — traces of morphology changes on the matrix surface; *c* — magnified image of a crater. The measurement mode parameters were as follows: the accelerating voltage 20 kV, the beam current 408 pA. An Everhart−Thornley secondary electron detector SE2 was used hereinafter, unless otherwise indicated.
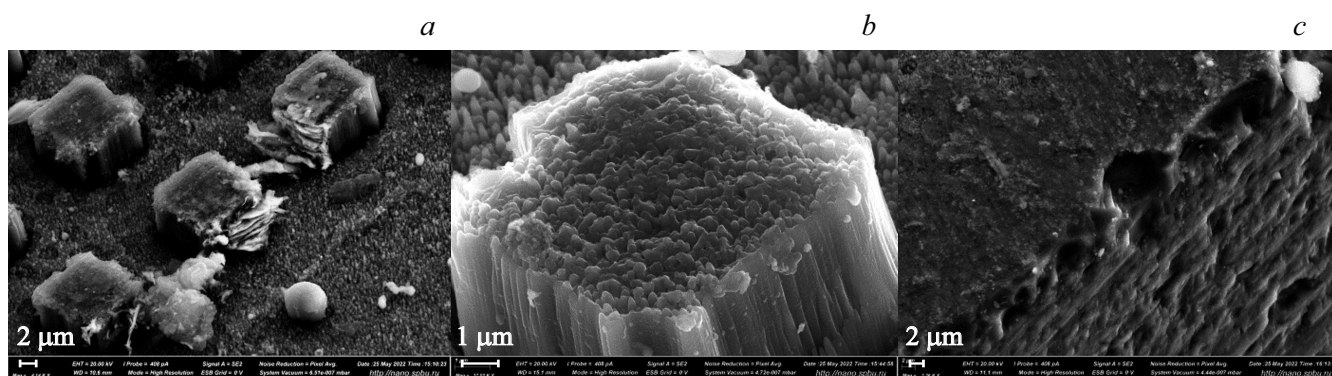

Figure 7. SEM image of elements of the silicon carbide matrix after the experiment: *a* — example of delamination of a pedestal with microtips; *b* — example of saving the structure of the operating surface on the pedestal; *c* — matrix edge.
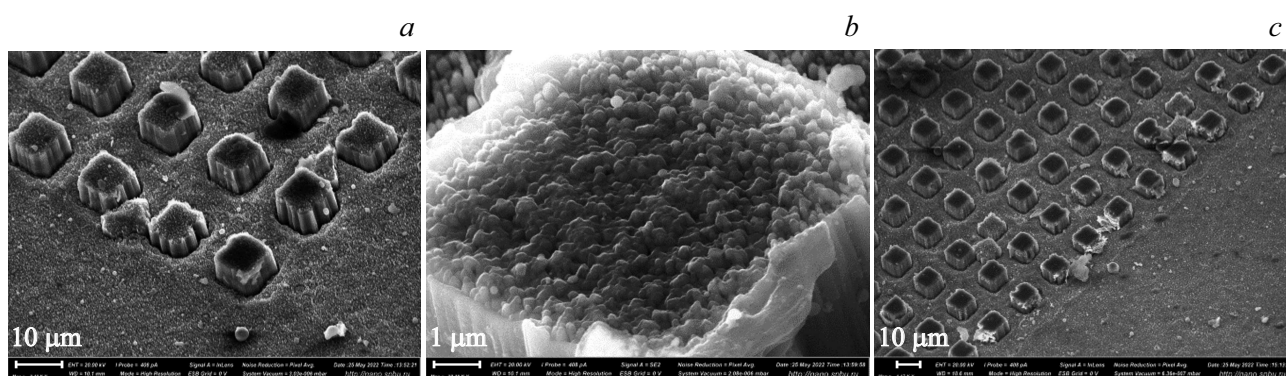

Figure 8. SEM image of the corner region of the matrix: *a* — the smoothed upper face of the corner element of the first scale level looks darker than the surface of the substrate and the low element adjacent to the left when using the In-Lens detector of secondary electrons; *b* — remnants of second scale level emission tips on the upper face of the corner element; *c* — smoothed top faces seem darker (In-Lens detector).

are presented, e.g., in [10]), which affects all smaller scale levels. Therefore, an increased value of the emission current density is expected in the region of edge, and especially, corner pedestals (details of the first scale level) on the matrix working surface. This was confirmed by the SEM image of the corner region of the cathode (Fig. 8). Firstly, the corner pedestal and the one adjacent to it on the left have a difference in height of $1-2\,\mu$m, therefore, due to screening of the field by higher neighbors, emission points of the second scale level have been
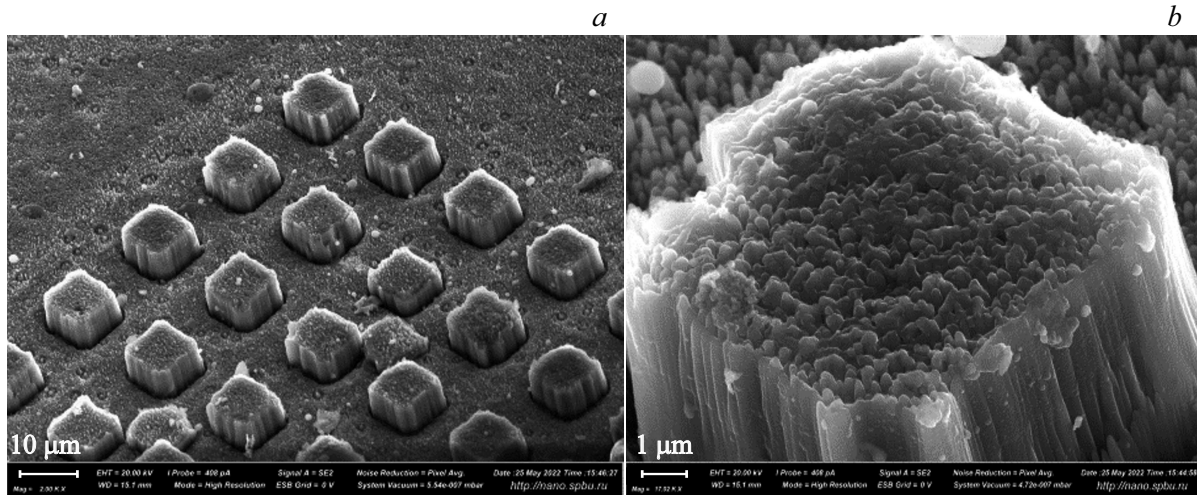
Figure 9. SEM image of the opposite corner of the matrix: *a* — general view of the neighborhood of the corner element of the first scale level, *b* — smoothing of the tips of the second scale level on the upper face of the corner element.

saved on the upper face of the lower pedestal (almost in the same state as on the substrate, and in the In-Lens detector, this face looks brighter, i.e., the contrast of the image emphasizes the difference in morphology, since this detector depicts a smoother surface with a darker color, Fig. 8, *a*).

Secondly, a spherical particle is visible on the substrate near the corner emitter; a more detailed image (Fig. 8, *b*) of the upper face of the corner emitter demonstrates the presence of balls also on the smoothed vertices of the tips.. Moreover, similar particles were observed in other parts of the matrix (Fig. 8, *c*). The chemical composition of the detected spherical particles was studied by X-ray spectral microanalysis (see the results below).

The SEM image of the diagonally opposite corner of the matrix (Fig. 9, *a*) shows a similar situation: the second-scale emission points are saved on the upper faces of the lower pedestals, while on the higher pedestals, including the corner ones, the smoothing of tips occurred (Fig. 8, *b* 9, *b* for comparison).

2.3. X-ray Spectral Microanalysis (XSMA)

An express analysis of the elemental composition of the sample was carried out using the detector of the system of energy dispersive X-ray elemental microanalysis (EDX, Oxford Instruments INCA x-act) in the same Zeiss Merlin microscope.

Let us consider the results of XSMA carried out in the vicinity of the corner element shown in Fig. 8. Spectra $1-8$ were recorded in a narrow local area (not quite at a point, since the penetration of the probing electron beam at an accelerating SEM voltage of $20\,\mathrm{kV}$ occurs to a depth of $1-7\,\mu\mathrm{m}$ in the material), as well as in a wider area, as shown in Fig. 10.
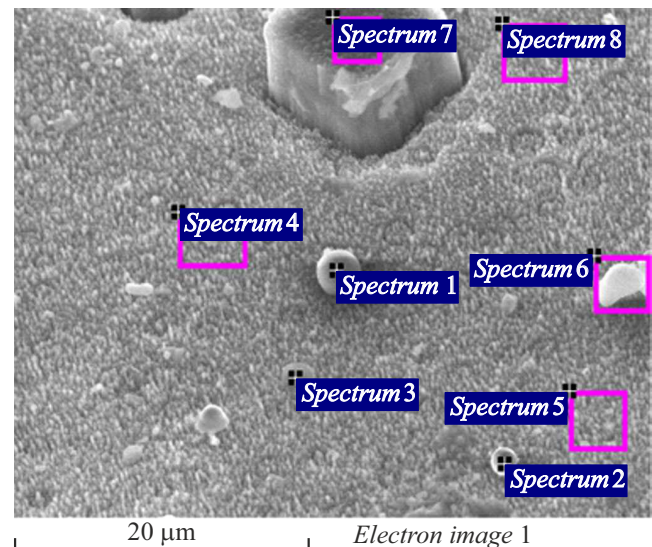

Figure 10. The location of the XSMA spectra measurement regions near the corner emission element shown in Fig. 8.

Spectrum *1* for a particle on the substrate shows a large amount of oxygen (O, 68.41 at.%) and the presence of aluminum (Al, 27.05 at.%), i.e. the spherical particle probably consists of oxidized aluminum, and a certain amount of Si and C is detected from the substrate due to the penetration of the electron beam deep into the material (in point measurement, this penetration by this and other small particles cannot be ignored). There is also molybdenum 0.35 at.% (or sulfur, since these elements are similar in XSMA, but the appearance of sulfur is unlikely in vacuum technology).

For another particle on the substrate, the spectrum *2* shows the presence of titanium (Ti, 3.15 at.%), a large amount of iron (Fe, 25.36 at.%) and copper (Cu, 1.32%).

Titanium was sputtered in particles (and even a thin film, as can be seen from spectrum *4*) possibly from titanium foil used to cut off the plasma plume, and Fe 0.02 at.%, probably, appeared from stainless steel of the vacuum chamber elements.

The spectrum *3* also shows the presence of molybdenum, 0.18 at.% (or sulfur). The spectrum *4* was recorded in the vicinity of a clean substrate (without visible deposited particles): a reduced content of silicon was found compared to carbon (Si, 19.30 at.% and C, 68.18 at.%, although these atoms should be in equal proportion in the volume of silicon carbide, but, probably, at higher temperature, partial graphitization occurs on the surface, since silicon leaves the crystal lattice during evaporation), and there is also Ti sputtered as a thin film (without visible particles) and Fe (the origin of these elements is suggested above).

The spectrum *6* of an irregularly shaped particle shows the presence of aluminum and oxygen, like in the balls, . In addition, there is Na, K, Ca, which could have arisen from some external pollution (the absence of carbon, characteristic of most pollution, is most likely due to an error in measurements or data processing algorithms).

The spectrum *7* was recorded on the upper face of the corner emitter in the region of smoothed tips: a low oxygen content is released (O only 5.76 at.%, i.e., the minimum compared to other spectra), and silicon and carbon are present in approximately the same amount as in other spectra (including those on the substrate).

The spectrum *8* was recorded on the substrate at the same angle as the spectrum *7* to check that the small amount of detectable oxygen in the spectrum *7* is not associated with a large viewing angle of the surface under study (near the edge of the field view of the x-ray detector). Two times more oxygen is detected on the substrate than on smoothed tips; therefore, during smoothing, the oxidized surface with a high oxygen content was removed and unoxidized silicon carbide emerged on the surface (from the bulk of the tips).

Conclusion

1. The functioning of a matrix cathode based on silicon carbide under conditions of pre-breakdown and breakdown in the mode of short high-voltage pulses in the range of voltage amplitudes $120-250$ kV has been studied.

2. The current-voltage characteristics of the matrix cathode are constructed.

3. An analysis of the CVCs plotted for the leading and trailing edge of the voltage and current pulses revealed their discrepancy, which may indirectly evidence for a change in the working surface of the cathode, including its morphology, at the leading edge of the voltage pulse.

4. Changes in the matrix structure affected not only the surface of the pedestals, but also penetrated deep into the basic substrate. The cathode under study operated in the explosive emission mode and the transition to it occurred at the highest tips or at the corners of the wafer.

5. During the experiment, both the edge of the matrix and its surface worked, which can be seen in the image of the cathode corner region. There is also a fairly high percentage of saved second-scale level emissive tips on the upper faces of lower pedestals, while on higher pedestals, including the corner ones, the tips were rounded, most likely due to the decomposition of the material during electron emission.

6. On the surface of the silicon carbide substrate, the presence of titanium was found, which was sputtered from a titanium foil used to cut off the plasma plume.

7. Two times more oxygen is detected on the substrate than on the smoothed tips; therefore, during smoothing, the oxidized surface with a high oxygen content was removed and unoxidized silicon carbide emerged from the volume of the tips to the surface.

Acknowledgments

Conflict of interest

The authors declare that they have no conflict of interest.

References

[1] V. Luchinin. Nanoindustry, **4** (65), 78 (2016).
DOI: 10.22184/1993-8578.2016.66.4.40.50

[2] A.V. Afanasyev, B.V. Ivanov, V.A. Ilyin, A.F. Kardo-Sysoev, M.A. Kuznetsova, V.V. Luchinin. Mater. Sci. Forum, **740−742**, 1010 (2013).
DOI: 10.4028/www.scientific.net/MSF.740-742.1010

[3] M.-G. Kang, H.J. Lezec, F. Sharifi. Nanotechnology, **24**, 065201 (2013). DOI: 10.1088/0957-4484/24/6/065201

[4] J.H. Choi, L. Latu-Romain, E. Bano, F. Dhalluin, T. Chevolleau, T. Baron. J. Phys. D: Appl. Phys., **45**, 235204 (2012).
DOI: 10.1088/0022-3727/45/23/235204

[5] L. Latu-Romain, M. Ollivier, V. Thiney, O. Chaix-Pluchery, M. Martin. J. Phys. D: Appl. Phys., **46**, 092001 (2013).
DOI: 10.1088/0022-3727/46/9/092001

[6] R. Wu, K. Zhou, J. Wei, Y. Huang, F. Su, J. Chen, L. Wang. J. Phys. Chem. C, **116** (23), 12940 (2012).
DOI: 10.1021/jp3028935

[7] H.C. Lo, D. Das, J.S. Hwang, K.H. Chen. Appl. Phys. Lett., **83**, 1420 (2003). DOI: 10.1063/1.1599967

[8] I.D. Evsikov, S.V. Mitko, P.Yu. Glagolev, N.A. Dyuzhev, G.D. Demin. ZhTF, **90** (11), 1931 (2020) (in Russian).
DOI: 10.21883/JTF.2020.11.49986.136-20 [I.D. Evsikov, S.V. Mit'ko, P.Yu. Glagolev, N.A. Djuzhev, G.D. Demin. Tech. Phys. **65** (11), 1846 (2020).
DOI:10.1134/S1063784220110067]

[9] N. Egorov, E. Sheshin. Field emission electronics. Springer Series in Advanced Microelectronics (2017), v. 60.
DOI: 10.1007/978-3-319-56561-3

[10] Nikiforov, K.A., Egorov, N.V. Saifullin, M.F. Tech. Phys. **60** (11), 1626 (2015).
DOI: 10.1134/S1063784215110225

[11] G.K. Kartsev, G.A. Mesyats, D.I. Proskurovskii, V.P Rotshtein, G.N. Fursei. Soviet Phys. Dokl., **15**, 475 (1970).

[12] V.A. Morozov, A.A. Lukin, G.G. Savenkov, I.A. Oskin. 2015 *International Conference „Stability and Control Processes" in Memory of V.I. Zubov* (SCP) (2015), p. 177−179.
DOI: 10.1109/SCP.2015.7342084

[13] N. Egorov, E. Sheshin, *Carbon-Based Field Emitters: Properties and Applications, in Vacuum Electron Sources*, ch. 10, G. Gärtner , W. Knapp, R.G. Forbes, Eds. (Springer, 2020)

Translated by Ego Translating